

On the Outage Probability of Multiuser Multiple Antenna Systems with Non-Orthogonal Multiple Access for Air-Ground Communications

Ayten Gürbüz, Giuseppe Caire (*Fellow, IEEE*), and Alexander Steingass

Abstract—This paper explores multiuser multiple antenna systems as a means to enhance the spectral efficiency of aeronautical communications systems. To this end, the outage regime for a multiuser multiple antenna system is studied within a realistic geometry-based stochastic air-ground (AG) channel model. In this application, users (aircraft) transmit air traffic management data to the ground station at a predefined target rate. Due to the nature of the AG propagation, we argue that the relevant performance metric in this context is the information outage probability. We consider the outage probability under three decoding approaches. The first is based on successive interference cancellation (SIC). The second extends the first approach by considering joint group decoding. The third is a version of the second that limits the size of the jointly decoded user groups in order to lower the decoding complexity. The results show that joint group decoding, even in groups of only two, can significantly increase the spectral efficiency in the AG channel by allowing a large number of aircraft to transmit over a non-orthogonal channel with very low outage probabilities.

Index Terms—Aeronautical communications, multipath channels, multiuser MIMO, NOMA, SIC, decoding order, joint decoding, outage probability

I. INTRODUCTION

ALL aircraft operating within a controlled airspace are managed by a globally standardized air traffic management (ATM) system to ensure the efficient traffic flow and flight safety. Air traffic controllers on the ground monitor the air traffic and give commands to the pilots on board the aircraft. In addition, they accept/reject requests from pilots to change their flight path. However, the demand for air transportation is continuously growing and the current systems are expected to reach their capacity in some world regions within the coming years [1]. Current aeronautical communications systems operate in the very high-frequency (VHF) band. Digital data links operating in the VHF band have been developed in the 1990s and only provide a limited data rate, well below the data rate required for a full ATM modernization in the future [2].

Ayten Gürbüz and Alexander Steingass are with the Institute of Communications and Navigation, German Aerospace Center (DLR), Oberpfaffenhofen, 82234 Weßling, Germany (e-mail: Ayten.Guerbuez@dlr.de; Alexander.Steingass@dlr.de).

Giuseppe Caire is with the Faculty of Electrical Engineering and Computer Science, Technical University of Berlin, 10587 Berlin, Germany (e-mail: caire@tu-berlin.de).

A key limitation in aeronautical communication technology is the spectrum to be used. Communications supporting ATM exchanges are classified as "safety of life" communications, which grants them special protection to prevent interference. However, this protection applies only to certain frequency bands in the VHF, L-band, and C-band [3]. Considering the congestion and propagation characteristics of these bands, the International Civil Aviation Organisation (ICAO) recommended the use of the frequency band between 960-1164 MHz in the L-band for the future aeronautical communications on a secondary basis [4], [5]. Operating on a secondary basis means that systems deployed in this band must not interfere with already existing legacy systems in the L-band. This imposes limits on the transmit power and spectrum usage. Therefore, the system must optimize the use of the limited spectrum while meeting the associated power constraints. To modernize the ATM system, two major research frameworks have been launched: the Single European Sky ATM Research (SESAR) [6] in Europe and the Next Generation National Airspace System [7] in the United States. Both researches are being conducted under the framework of ICAO.

The growing demands of aeronautical communications can be addressed by multiple antenna systems, which are known to improve spectral efficiency. In [8], we presented achievable upper boundaries for a single-user multiple antenna system and demonstrated that the performance is limited by the propagation characteristics of the air-ground (AG) communications. An alternative to point-to-point multiple antenna systems is a multiuser system, [9]–[12], where an antenna array receives signals from multiple users simultaneously. In this case, the users are not separated in time or frequency; this is known as non-orthogonal multiple access (NOMA). Multiuser systems are more resilient to the propagation environment, allowing them to exploit the full potential of multiple antenna technology.

Multiuser multiple antenna systems have been extensively studied in cellular communications. In addition, numerous studies investigate the use of unmanned aerial vehicles and/or satellites to support ground networks in cellular communications, e.g. [13]–[15]. However, the vehicles in these studies differ significantly in speed and altitude, leading to different propagation characteristics. Moreover, current studies do not consider "safety of life" applications such as the one we are investigating. As a result, we cannot directly rely on these studies, as our work involves different propagation characteristics and stricter constraints due to the critical nature

This work has been submitted to the IEEE for possible publication. Copyright may be transferred without notice, after which this version may no longer be accessible.

of the ATM communications systems. Research on multiuser multiple antenna systems with NOMA for ATM systems, especially for aircraft traveling long distances at high speeds, is limited, with [16] being, to the best of our knowledge, one of the few available studies. However, this study does not thoroughly consider the realistic propagation characteristics of the AG channel and focuses solely on the achievable ergodic sum rate [17].

The propagation characteristics of the AG channel have been extensively studied through measurement campaigns [18]–[20]. In this study, we adapt the geometry-based stochastic AG channel model from [21], which was developed based on the measurement campaign in [18]. Originally designed for a single antenna system, we extend it to a multiple antenna system with NOMA setup using the insights from [22] and derive the corresponding channel matrix.

Due to the strict nature of the ATM systems, the constraints considered in this paper are as follows: the aircraft's transmission power is fixed according to the SESAR project specifications [6], [23], aligning with the power limits of the protected L-band. This fixed transmission power is necessary to maintain simplicity in the onboard system. For the same reason, we also assume a single antenna element on the aircraft. On the other hand, we consider an antenna array at the ground station (GS). All aircraft in the system must meet the guaranteed rate to ensure the reliable transmission of flight critical messages. We consider two cases: a) an equal-rate system in which all aircraft transmit at the system's guaranteed rate, and b) a variable-rate system, where aircraft transmit at least at the guaranteed rate.

Using the extended channel model and considering the constraints and requirements of aeronautical communications systems, this paper focuses on the fundamental research of multiuser multiple antenna technology for AG communications. The main contributions are listed as follows:

- We study the multiuser multiple antenna system technology with NOMA within a realistic geometry-based stochastic AG channel model and motivate the outage regime.
- We evaluate the outage probability under three decoding algorithms. These algorithms minimize the outage probability for either only successive interference cancellation (SIC) decoders or SIC decoders in conjunction with joint group decoding.
- The first algorithm is the single successive algorithm (SSA), which minimizes the outage probability for SIC decoders. We compare SSA with the decoding order strategies proposed in [24] and [25]. We show that SSA outperforms the decoding ordering strategy in [25]. Moreover, we prove that the vertical-bell laboratories layered space-time (V-BLAST) algorithm [24] finds an optimal solution that minimizes the outage probability in equal-rate systems but it cannot obtain an optimal decoding order in variable-rate systems. Hence, SSA outperforms V-BLAST in variable-rate systems.
- The second algorithm is the group successive algorithm (GSA). It determines the minimum achievable outage probability for a given capacity region. To achieve this

minimum outage probability, it is necessary to use the SIC decoders together with joint group decoders. GSA significantly reduces the outage probability compared to SSA. The difference between GSA and SSA becomes more apparent when the number of transmitting aircraft is large.

- The third algorithm is the limited group successive algorithm (LGSA). It is a version of GSA that forces the joint group decoding to be done in small groups. It does not obtain the optimal solution like GSA, but it provides a more feasible solution for real-world applications while still proposing a significant improvement over SSA.

Subsequently, the paper is organized as follows: in Section II, we introduce the fixed parameters of the system. In Section III, we first provide background on the AG channel propagation, and follow this with an introduction to the channel model used in the simulations. Moving to Section IV, we explore the interplay between the capacity region and outage probability and demonstrate that the calculation of the outage probability is a challenging problem. In Section V, we propose algorithms to solve the posed problems in Section IV. Subsequently, in Section VI, we present two existing decoding ordering algorithms in the literature. Proceeding to Section VII, we evaluate the performance and computational complexity of the proposed algorithms and compare their performance with the existing decoding order algorithms in the literature. Finally, in Section VIII we summarize the obtained results and give an outlook for the future.

II. SYSTEM MODEL

In this work, we study a communications system between a GS and multiple aircraft. The GS has an antenna array consisting of M antenna elements, while each of the K aircraft is equipped with a single antenna. In order to meet the constraints of the protected L-band spectrum for ATM communications, the system model parameters are chosen based on the specifications in [23]. We assume that all K aircraft transmit simultaneously to the GS, at the carrier frequency of 987 MHz [23]. Thus, we consider a multiuser multiple antenna system with NOMA in the reverse link. To comply with the transmit power constraints, the transmit power of each aircraft is set to $P = 41$ dBm, and the noise power at each receiver antenna is assumed to be $N_0 = -107$ dBm [23].

Furthermore, in this work a curved Earth model with a radius of 6371 km is used [26]. The GS is assumed to be at the center of a circular cell with a radius of 222 km (120 nautical miles) [23] and positioned 500 m above the mean sea level (MSL), as tested in [18], [27]. In this paper, we focus only on the enroute cruise (EC) scenario. To this end, the altitude of the K aircraft is set at 10 km above MSL, a typical altitude for commercial flights, which corresponds to above flight level 300 [28]. Based on Instrument Flight Rules [28], we maintain a minimum separation of 10 km (approximately 5 nautical miles) between any two aircraft to ensure realistic spacing and avoid overlap. We repeatedly simulate the positions of the aircraft within the given constraints to calculate the outage probability.

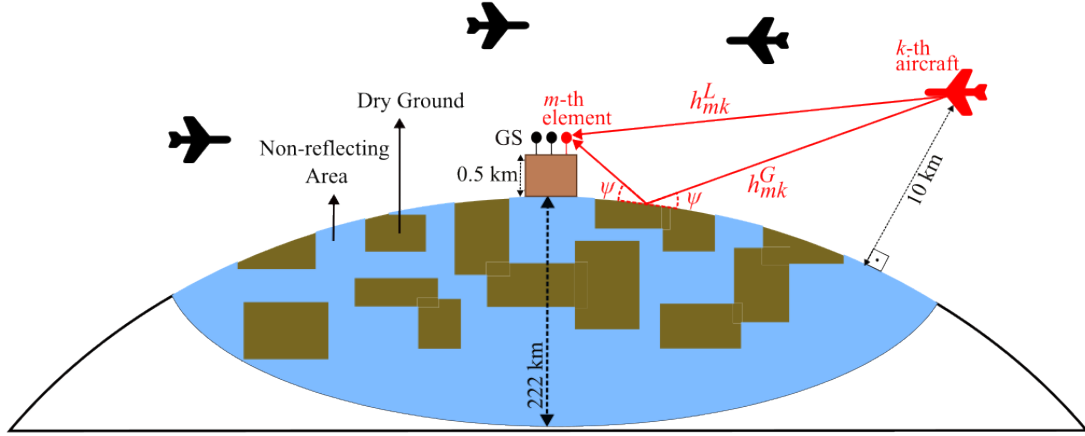


Fig. 1. Simulation setup illustrating the system and channel model

The evaluations are performed for a uniform planar rectangular array (UPRA) where the antenna elements are arranged in a $\sqrt{M} \times \sqrt{M}$ grid, with each element evenly spaced at half-wavelength intervals. We assume that the antenna elements have an isotropic radiation pattern and that the mutual coupling between the array elements is neglected, which is a common assumption in the literature on multiuser multiple antenna systems [9]–[12].

III. AIR-GROUND PROPAGATION AND CHANNEL MODEL

An understanding of the propagation effects is crucial for accurately modeling a realistic channel. In this section, we first provide a summary of the air-ground propagation insights based on the measurement campaigns conducted in the L-band AG channel [18]–[20]. Following this, we describe how we utilize the AG channel model presented in [21].

A. Air-Ground Propagation

According to the measurement campaigns [18]–[20] the most dominant multipath component (MPC) in the L-band AG channel is the line-of sight (LOS) path, which is the direct path between the aircraft and the GS. The LOS path has significantly higher power than the other MPCs and that it is almost always present.

The second strongest MPC is the ground reflection, also called the ground multipath component (GMP). This is a specular reflection (SR) where the reflecting point is located on the direct line between the projection of GS and the projection of the aircraft on the ground. The GMP reaches the receiver shortly after the LOS signal and with a very similar Doppler frequency compared to the LOS signal. Therefore, it interferes constructively or destructively with the LOS. In [18], LOS attenuations of up to 20 dB and amplifications of up to 6 dB have been reported as a result of the GMP. The presence and power of the GMP depends on the terrain. For instance, when the aircraft flies over water, a strong GMP is typically observed [19], while over hilly or mountainous terrain, the GMP is present only during certain parts of the flight. This is due to the roughness of the ground, which not only reflects but also scatters the signal, reducing the energy reaching the receiver [20].

The MPCs that reflect off buildings, large structures, or vegetation are known as lateral multipath components (LMPs). These reflectors are usually located near the GS. The LMPs typically have much lower power than both LOS and GMP.

Fading channels, which result from the constructive and destructive superposition of the various propagation paths, are known to have fluctuations. Each fluctuation lasts a certain length of time. This duration, also known as the "coherence time", is approximately inversely proportional to the Doppler spread, which is defined as the difference between the maximum and minimum Doppler frequency shifts. The measurement results in [18] indicate that the Doppler spread of the AG channel is significantly affected by the altitude, speed, and distance of the aircraft from the GS. The three main phases of a typical flight scenario are takeoff & landing (TL), climb & descent (CD), and EC. These phases have different propagation characteristics. In the EC phase, all propagation paths experience the same Doppler shift as the LOS path due to large distance between the transmitter and receiver and the resulting geometry. This leads to a very small Doppler spread. Consequently, the coherence time is large, resulting in a long period of deep fades. In the CD, the Doppler spread is slightly larger than in the EC phase. According to [29], which is also based on the measurement campaign reported in [18], the Doppler spread in this phase is 60 Hz. In the TL phase the Doppler spread is much higher, resulting in shorter coherence time.

In this paper we consider only the EC scenario, where the aircraft flies at an altitude of 10 km, above flight level 300 [28], and maintains a high average speed. The exact Doppler spread of the channel in this scenario is not documented in [18], [29]. However, it is known to be smaller than in the CD phase, which is 60 Hz. Therefore, we can estimate that the coherence time of the channel in the EC scenario is at least $1/60 \text{ Hz} = 16 \text{ ms}$. Taking the example of the SESAR system specifications, in [23] it is indicated that the duration of each codeword for aircraft to GS transmission varies between 0.72 ms to 7.2 ms, depending on the modulation scheme, coding rate, and resource requirements of the aircraft. Since the coherence time of the channel is at least 16 ms in the EC phase, it is reasonable to consider the channel as random

but constant over a whole codeword, in accordance with the "capacity versus outage approach" introduced in [30] for the so-called "block-fading channel".

B. Channel Model

In this work, we utilize a simplified version of the proposed geometry-based stochastic channel model for the AG channel in [21]. The channel model parameterization is based on an L-band airborne measurement campaign that took place at a regional airport in 2013, which is described in detail in [18]. Building on this geometry-based stochastic channel model, we consider only the two strongest propagation effects in [21]: the LOS and the GMP. We assume that the LOS is always present and that it is modelled as the shortest possible path between the aircraft and the GS. The presence of the GMP, however, depends on the position of the aircraft.

The GMP propagation effect is modeled by randomly characterizing the reflecting and non-reflecting areas on the ground. Figure 1 shows an example ground reflecting area realization in the channel model. In the simulations, the ratio between the total area of all reflecting surfaces and the overall area around the GS is 50%, as it is approximated in [21] for a regional airport environment. A GMP is present when the ground reflection point falls within a reflecting area. The location of the ground reflector is determined by calculating the SR point on the ground surface, which depends on the coordinates of both the GS and the aircraft [31]. The reflective areas are modeled as rectangles, with their size always much larger than the wavelength of the carrier signal. In [21], the reflective surfaces are modeled as concrete, dry ground, and medium ground, based on the measurement campaign in [18]. In our study, for simplicity, we model the reflective surfaces as dry ground only.

As justified in Section III-A, the channel can be treated as a random variable rather than a process for each codeword transmission [30]. To this end, we compute the instantaneous realization of the channel based on the positions of the K aircraft. The LOS, h_{mk}^L , and the GMP, h_{mk}^G , channels between the m -th antenna element and the k -th aircraft are each computed as

$$h_{mk}^L = \alpha_{mk}^L \cdot \exp\left(-j2\pi \frac{d_{mk}^L}{\lambda}\right), \quad (1)$$

$$h_{mk}^G = \rho_v \cdot \alpha_{mk}^G \cdot \exp\left(-j2\pi \frac{d_{mk}^G}{\lambda}\right). \quad (2)$$

The path strengths for these channels are denoted by α_{mk}^L and α_{mk}^G , respectively. These values are calculated using the free-space path loss (FSPL) formula. The propagation path lengths for these channels are given by d_{mk}^L and d_{mk}^G , the phase of the signals calculated by using the path lengths, and the signal wavelength, λ . The vertical reflection coefficient for the GMP is denoted by ρ_v , which equals 0 when the ground reflection point lies within a non-reflective area. If the ground reflection point is in a reflective area, ρ_v is calculated using the equation from [31], which considers the grazing angle and the electromagnetic properties of dry ground as specified in [32].

In the end, the channel between the m -th antenna element and the k -th aircraft, h_{mk} , is calculated by

$$h_{mk} = h_{mk}^L + h_{mk}^G. \quad (3)$$

The vector representing the channel between the antenna array on GS and the k -th aircraft is then given by $\mathbf{h}_{:k} = [h_{1k}, h_{2k}, \dots, h_{Mk}]^T \in \mathbb{C}^M$, and the channel matrix between the K aircraft and the GS is $\mathbf{H} = [\mathbf{h}_{:1}, \mathbf{h}_{:2}, \dots, \mathbf{h}_{:K}] \in \mathbb{C}^{M \times K}$.

IV. CAPACITY REGION AND OUTAGE PROBABILITY

The signal received at GS for *one channel use* of the discrete-time baseband complex channel model is denoted as $\mathbf{y}_j \in \mathbb{C}^M$ and it is related to the channel matrix $\mathbf{H} \in \mathbb{C}^{M \times K}$ by

$$\mathbf{y}_j = \mathbf{H}\mathbf{x}_j + \mathbf{z}_j, \quad j = 1, \dots, n \quad (4)$$

where $\mathbf{x}_j \in \mathbb{C}^K$ is the vector of channel input symbols transmitted by the K aircraft, $\mathbf{z}_j \in \mathbb{C}^M$ is a complex Gaussian noise $\mathcal{CN}(0, N_0 \mathbf{I}_M)$, and n is the codeword length. As explained before, the channel matrix \mathbf{H} is constant over the transmission of one codeword, i.e., during n channel uses. In this work, we assume that \mathbf{H} can be perfectly estimated at the receiver.

A. Capacity Region

From an information-theoretic point of view, the channel with K aircraft and one receiver, i.e., GS, with M receiving antennas and a fixed channel matrix \mathbf{H} is a vector Gaussian multiple-access channel (MAC). An achievable rate K -tuple is a vector of rates (R_1, R_2, \dots, R_K) that can be simultaneously transmitted by the users with arbitrarily small probability of error [33]. The capacity region \mathcal{C}_{MAC} is the convex closure of the set of all achievable rates. From [34, p. 425], under the assumption that all K aircraft transmit at a fixed power P , and that each receiver antenna has a noise power N_0 the capacity region is given by

$$\mathcal{C}_{\text{MAC}} = \left\{ (R_1, R_2, \dots, R_K) : \sum_{k \in S} R_k \leq \dots \right. \\ \left. \log_2 \det \left(\mathbf{I}_M + \frac{P}{N_0} \mathbf{H}_{:S} \mathbf{H}_{:S}^H \right), \forall S \subseteq \{1, 2, \dots, K\} \right\}, \quad (5)$$

where $\mathbf{H}_{:S}$ is the submatrix obtained from \mathbf{H} by taking the columns $\{\mathbf{h}_{:k} : k \in S\}$ and the superscript H refers to the conjugate transpose. From the converse result on the capacity region and the arguments in [30], for any coding scheme transmitting at rates $\mathbf{R} = (R_1, R_2, \dots, R_K)$, if \mathbf{H} is such that $\mathbf{R} \notin \mathcal{C}_{\text{MAC}}$, then the probability that some aircraft messages are decoded in error is close to 1.

For example, consider two arbitrary channel matrices with $K = 2$, the corresponding rate regions for each channel matrix realization are shown in Fig. 2. In both rate regions, the rate A is the achievable rate for aircraft 1 in the absence of interference from aircraft 2, and B is the achievable rate for aircraft 2 in the absence of interference from aircraft 1. In contrast, R_1^2 and R_2^1 are the achievable rates for aircraft 1 and

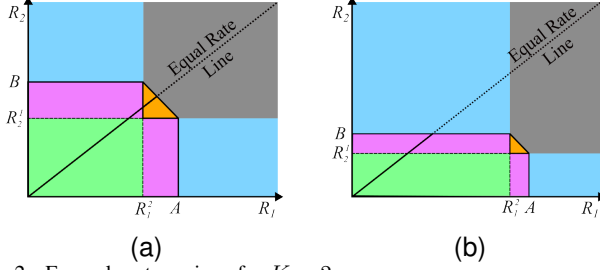


Fig. 2. Example rate regions for $K = 2$

2, respectively, when the decoder at the GS is treating the interference as noise.

The pink, orange, and green areas are within the capacity region. In Fig. 2a, the capacity region is highly symmetric, indicating that the achievable rates for both aircraft are quite similar. In contrast, Fig. 2b shows a strongly asymmetric capacity region. Such asymmetry typically results from a strong power imbalance in the signals received from different aircraft. In AG communications, this situation is likely to occur due to large distance differences between the aircraft and the GS. Therefore, cases with highly asymmetric capacity regions cannot be neglected.

Of particular interest are the so-called "corner points" of the capacity region, corresponding to the points (A, R_2^1) and (R_1^2, B) . These points are on the "dominant face" of the capacity region and are therefore sum rate optimal. The following equality holds for these points

$$R_1^2 + B = A + R_2^1 = \log_2 \det \left(\mathbf{I}_M + \frac{P}{N_0} \mathbf{H} \mathbf{H}^H \right). \quad (6)$$

It is well known that these corner rate points can be achieved by a particularly simple decoding scheme known as SIC decoding. For example, the point (A, R_2^1) can be achieved by first decoding user 2 while treating the interference from user 1 as noise, and then subtracting the codeword of user 2 from the received signal. Since the probability of error of user 2 at rate R_2^1 is vanishing, SIC can (almost) perfectly remove the interference, such that the decoder for user 1 operates on a clean channel. Therefore, the rate A can be achieved for user 1, since at this point the decoder sees an interference-free channel.

B. Outage Event Identification

Aircraft k transmits at rate r_k and the system's guaranteed rate is r_G . We consider two cases for $\forall k \in \{1, 2, \dots, K\}$: the first is the *equal-rate system*, where $r_k = r_G$, and the second is the *variable-rate system*, where $r_k \geq r_G$. To determine which aircraft can reliably transmit, i.e., which aircraft are not in outage, we need to examine the capacity region. For example, when $K = 2$, the rate point is denoted as (r_1, r_2) . In an equal-rate system, the rate point $(r_1, r_2) = (r_G, r_G)$ is on the equal-rate line shown in Fig. 2. On this line, the solid portion represents the regions within the capacity region, while the dashed portions indicate areas outside the capacity region. By examining the position of any given rate point on the rate region, we can determine which aircraft's transmitted signals can be successfully decoded. Additionally, the color

of the region indicates the decoding technique required, such as independent single-user (ISU) decoders, SIC decoders, or joint group decoders. In particular:

- In the green area, both signals can be decoded separately using ISU decoders by treating the interference as noise.
- Inside the pink areas, both signals can be decoded using a SIC scheme [33]. It is important to select the correct decoding order to ensure that both transmitted signals are successfully decoded. For example, if $R_2^1 < r_2 \leq B$ and $r_1 \leq R_1^2$, then we must first decode aircraft 1 and then aircraft 2.
- Within the orange area, joint group decoding becomes necessary, where the transmitted signals are decoded together as a group. This process is more complex to implement in practice.
- In the blue areas, the rate vector is not in the capacity region. However, one of the transmitted signals can still be decoded by treating the other signal as noise. The specific blue area where the rate point is located determines which aircraft will be in outage. For example, if $B < r_2$ and $r_1 \leq R_1^2$ then aircraft 2 will be in outage but aircraft 1 will not.
- Inside the gray area, both aircraft will be in outage.

As a result, if the rate point is outside the capacity region, it does not necessarily mean that all transmitting aircraft are in outage.

C. Outage Probability

To calculate the probability of outage, we need to find the largest set of aircraft $S^* \subset \{1, 2, \dots, K\}$ such that $\forall k \in S^*$ can be decoded at rate r_k . Consequently, the complementary set, $\hat{S} \subset \{1, 2, \dots, K\}$, where $S^* \cap \hat{S} = \emptyset$, represents the set of aircraft in outage. Accordingly, the outage probability, P_{out} , is

$$P_{\text{out}} = 1 - \frac{\mathbb{E}[|S^*|]}{K} = \frac{\mathbb{E}[|\hat{S}|]}{K}, \quad (7)$$

where $\mathbb{E}[\cdot]$ denotes the expectation with respect to the realizations of the random channels \mathbf{H} , and is evaluated by Monte Carlo simulation for the model defined in Section II.

Our goal is to minimize the outage probability. This is accomplished by finding the set S^* of maximum size for each realization of the channel matrix \mathbf{H} . Hence, for a given rate point (r_1, \dots, r_K) and a given \mathbf{H} , we wish to find

$$\max |S^*|. \quad (8)$$

In particular, it follows from (5) that S^* is the maximal set satisfying the condition:

$$\forall S \subseteq S^*,$$

$$\sum_{k \in S} r_k \leq \log_2 \det \left(\mathbf{I}_M + \dots \right) \quad (9)$$

$$\frac{P}{N_0} \mathbf{H}_{:\hat{S}} \mathbf{H}_{:\hat{S}}^H \left(\mathbf{I}_M + \frac{P}{N_0} \mathbf{H}_{:\hat{S}} \mathbf{H}_{:\hat{S}}^H \right)^{-1} \right),$$

where $\mathbf{H}_{:\hat{S}}$ is the matrix representing the aircraft that are in outage, with columns $\{\mathbf{h}_{:k} : k \in \hat{S}\}$.

Finding the maximal set S^* becomes more challenging as the number of aircraft in the system, K , increases. A brute-force approach to derive S^* requires considering every possible combination of $[K] = \{1, 2, \dots, K\}$. Additionally, for each combination, we must evaluate all non-empty subsets, which amounts to $(2^v - 1)$ subsets for a combination of v aircraft. This results in a total of

$$\begin{aligned} & \sum_{v=1}^K \sum_{S^* \in \binom{[K]}{v}} (2^v - 1) \\ &= \sum_{v=1}^K \frac{K!}{v!(K-v)!} (2^v - 1), \end{aligned} \quad (10)$$

which is the number of times we need to compute the condition given in (9) in order to derive S^* .

D. Outage Probability for SIC decoders

The outage probability for SIC decoders means that the solution space is limited by the exclusion of joint group decoding. The largest set of non-outage aircraft under the SIC scheme is defined as S_{SIC}^* , where S_{SIC}^* is a subset of S^* . Accordingly, the outage probability for SIC decoders is $P_{\text{out}}^{\text{SIC}} = 1 - \frac{\mathbb{E}[|S_{\text{SIC}}^*|]}{K}$, where $P_{\text{out}}^{\text{SIC}} \geq P_{\text{out}}$.

Let $i_1 \rightarrow i_2 \rightarrow \dots \rightarrow i_K$ be a permutation of the integers $1, 2, \dots, K$ representing the decoding order. We define $R_{i_u}^{T_u}$ as

$$\begin{aligned} R_{i_u}^{T_u} &= \log_2 \det \left(\mathbf{I}_M + \dots \right. \\ &\quad \left. \frac{P}{N_0} \mathbf{h}_{i_u} \mathbf{h}_{i_u}^H \left(\mathbf{I}_M + \frac{P}{N_0} \mathbf{H}_{:T_u} \mathbf{H}_{:T_u}^H \right)^{-1} \right), \end{aligned} \quad (11)$$

where $\mathbf{H}_{:T_u}$ denotes the matrix formed by the columns $\{\mathbf{h}_{i_k} : k > u\}$ and $u \in \{1, 2, \dots, K\}$. In this context, we define the set S_{SIC}^* as

$$\begin{aligned} S_{\text{SIC}}^* &= \{i_1, \dots, i_{u^*-1} : \dots \\ &\quad u^* = \min_{u \in \{1, \dots, K\}} u \text{ subject to } r_{i_u} > R_{i_u}^{T_u}\}, \end{aligned} \quad (12)$$

where u^* is the smallest index for which the outage condition, $r_{i_{u^*}} > R_{i_{u^*}}^{T_{u^*}}$, holds. If none of the aircraft are in outage, i.e., $r_{i_u} \leq R_{i_u}^{T_u}, \forall u \in \{1, \dots, K\}$, then we assume that $\min_{u \in \{1, \dots, K\}} u = K + 1$ in (12), such that the cardinality of the set S_{SIC}^* is K . Thus, the size of the S_{SIC}^* depends on the decoding order. In order to minimize the outage probability, the optimization problem is formulated as

$$\max_{\Pi} |S_{\text{SIC}}^*|, \quad (13)$$

where Π represents the decoding order. A brute-force approach to find an optimal decoding order that maximizes the size of S_{SIC}^* requires evaluating all $K!$ permutations, which becomes computationally very expensive as K increases.

In the rest of the paper, for arbitrary values of x and y , the notation R_x^y means the achievable rate of x under the interference of y , and it is calculated by the right hand side (RHS) of (11) where i_u is defined by x and T_u is defined by y .

Lemma IV.1. Let T_o and T_p be two distinct sets, where $o \notin T_o$ and $p \notin T_p$. If $o = p$ and $T_o \subset T_p$, then it follows that $R_o^{T_o} \geq R_p^{T_p}$ [24].

Proof. The sets T_o and T_p represent the interfering aircraft with o and p , respectively. According to Shannon's capacity equation, an increase in interference leads to lower achievable data rate. As a result, as more aircraft interfere with the transmitted signal, the achievable data rate will either remain the same or decrease, depending on the linear dependence of the channel vectors associated with the aircraft. \square

E. Outage Probability for ISU decoders

ISU decoders decode the signals from each aircraft separately. For example, well-known zero forcing (ZF) and minimum mean squared error (MMSE) decoders are examples of ISU decoders [34]. When decoding aircraft k , an ISU decoder treats the interference from the other aircraft as noise. Accordingly, the non-outage condition for aircraft k is

$$r_k \leq \log_2 \det \left(\mathbf{I}_M + \frac{P}{N_0} \mathbf{h}_{:k} \mathbf{h}_{:k}^H \left(\mathbf{I}_M + \frac{P}{N_0} (\mathbf{H})_k (\mathbf{H})_k^H \right)^{-1} \right), \quad (14)$$

where the notation $(\mathbf{H})_k$ represents the removal of the k -th column from \mathbf{H} . The largest set of non-outage users using ISU decoders is defined as S_{ISU}^* . Accordingly, the upper-bound on the minimal outage probability for ISU decoders is $P_{\text{out}}^{\text{ISU}} = 1 - \frac{\mathbb{E}[|S_{\text{ISU}}^*|]}{K}$, where $P_{\text{out}}^{\text{ISU}} \geq P_{\text{out}}^{\text{SIC}} \geq P_{\text{out}}$.

V. PROPOSED ALGORITHMS FOR CALCULATING OUTAGE PROBABILITY

We have shown in the previous section that the optimization problems given in (8) and (13) are difficult to solve with a brute force approach due to the associated high computational complexity. In this context, we propose three algorithms designed to efficiently identify solutions while significantly reducing the computational complexity. These algorithms not only compute an upper bound on the minimal outage probability, but also provide practical achievability strategies. As such, they provide explicit decoding orders for SIC and SIC with joint group detection in subgroups that can be implemented in a practical receiver. The first algorithm is SSA, this aims to solve the problem given in (13). SSA identifies the largest subset of decodable aircraft by excluding the joint group decoding options. The second algorithm is GSA, which extends SSA by using its outputs as inputs. GSA solves the problem in (8), where joint group decoding options are included. The third algorithm is LGSA, which is a modified version of GSA. With LGSA we find a suboptimal solution to the problem in (8) by limiting the number of aircraft that can be decoded jointly.

The complexity of the problems given in (8) and (13) is reduced by starting the evaluation from the smallest subsets and using the insights gained from these evaluations. This allows us to eliminate certain subset options or decoding orders from further consideration, thereby narrowing the search space and improving computational efficiency. There are three sets in the

Algorithm 1 Single Successive Algorithm (SSA)**Input:** $\mathbf{H}, \mathbf{r} = (r_1, \dots, r_K)$ **Output:** S^*, \hat{S}, L **Initialization**1: $L = \{1, 2, \dots, K\}, S^* = \emptyset, \hat{S} = \emptyset$ **Phase 1 - Prune Aircraft**

```

2: function PRUNEAIRCRAFT( $\mathbf{H}, \mathbf{r}, L, \hat{S}$ )
3:   while  $|L| > 0$  do
4:      $\text{tmp} = \hat{S}$ 
5:     for each  $l \in L$  do
6:        $R_l^{\hat{S}} = \log_2 \det \left( \mathbf{I}_M + \dots \right.$ 

$$\left. \frac{P}{N_0} \mathbf{h}_l \mathbf{h}_l^H \left( \mathbf{I}_M + \frac{P}{N_0} \mathbf{H}_{:\hat{S}} \mathbf{H}_{:\hat{S}}^H \right)^{-1} \right)$$

7:       if  $r_l > R_l^{\hat{S}}$  then
8:         Remove  $l$  from  $L$ 
9:          $\hat{S} \leftarrow \text{add } l$ 
10:      if  $\text{isequal}(\text{tmp}, \hat{S})$  then break
11:   return  $L, \hat{S}$ 

```

Phase 2 - Greedy SIC

```

12: function GREEDYSIC( $\mathbf{H}, \mathbf{r}, L, S^*, \hat{S}$ )
13:   while  $|L| > 0$  do
14:      $\text{tmp} = S^*$ 
15:     for each  $l \in L$  do
16:        $T_l = (L \cup \hat{S}) \setminus \{l\}$ 
17:        $R_l^{T_l} = \log_2 \det \left( \mathbf{I}_M + \dots \right.$ 

$$\left. \frac{P}{N_0} \mathbf{h}_l \mathbf{h}_l^H \left( \mathbf{I}_M + \frac{P}{N_0} \mathbf{H}_{:T_l} \mathbf{H}_{:T_l}^H \right)^{-1} \right)$$

18:       if  $r_l \leq R_l^{T_l}$  then
19:         Remove  $l$  from  $L$ 
20:          $S^* \leftarrow \text{add } l$ 
21:       if  $\text{isequal}(\text{tmp}, S^*)$  then break
22:   return  $L, S^*$ 

```

algorithms: S^* , \hat{S} , and L . These three sets form a partition of $\{1, 2, \dots, K\}$. The set S^* contains aircraft that can be successfully decoded at their transmission rate, i.e., $\forall k \in S^*$ can be decoded at the rate r_k . Set \hat{S} contains the aircraft that are certainly in outage and L contains the aircraft whose status has not yet been determined. As the algorithms progress, the aircraft that can be decoded successfully or are known to be in outage are removed from L and added to either S^* or \hat{S} . Thus, the objective of the algorithms is to minimize the set L by removing as many elements as possible. The aircraft that cannot be removed from L at the end of the algorithms can be considered as being in outage, since no solution could be found to successfully decode them.

A. Single Successive Algorithm (SSA)

SSA is presented in Algorithm 1 and solves the optimization problem given in (13). Please note that S_{SIC}^* in (13) is denoted by S^* in this algorithm. We start by setting $L = \{1, 2, \dots, K\}$, $S^* = \emptyset$, and $\hat{S} = \emptyset$, and then move the aircraft from L to either S^* or \hat{S} during two main phases.

The first phase is referred to as *PruneAircraft*. It identifies aircraft that are definitely in outage. Consider $l \in L$, in line 6, $R_l^{\hat{S}}$ is defined as the achievable rate of aircraft l under the

Algorithm 2 Group Successive Algorithm (GSA)**Input:** $\mathbf{H}, \mathbf{r} = (r_1, \dots, r_K)$ **Output:** S^*, \hat{S}, L **Phase 1 - Single Successive Algorithm**

```

1:  $L = \{1, 2, \dots, K\}, S^* = \emptyset, \hat{S} = \emptyset$ 
2:  $L, \hat{S} \leftarrow \text{PRUNEAIRCRAFT}(\mathbf{H}, \mathbf{r}, L, \hat{S})$ 
3:  $L, S^* \leftarrow \text{GREEDYSIC}(\mathbf{H}, \mathbf{r}, L, S^*, \hat{S})$ 

```

Phase 2 - Prune Subsets

```

4: while  $|L| \geq 2$  do
5:    $\text{tmp} = \hat{S}$ 
6:    $\text{Combinations} = \binom{L}{2}$ 
7:   for each  $C \in \text{Combinations}$  do
8:      $R_C^{\hat{S}} = \log_2 \det \left( \mathbf{I}_M + \dots \right.$ 

$$\left. \frac{P}{N_0} \mathbf{h}_{:C} \mathbf{h}_{:C}^H \left( \mathbf{I}_M + \frac{P}{N_0} \mathbf{H}_{:\hat{S}} \mathbf{H}_{:\hat{S}}^H \right)^{-1} \right)$$

9:     if  $\sum_{k \in C} r_k > R_C^{\hat{S}}$  then
10:       Remove  $C$  from  $L$ 
11:        $\hat{S} \leftarrow \text{add } C$ 
12:     break
13:   if  $\text{isequal}(\text{tmp}, \hat{S})$  then break
14:    $L, \hat{S} \leftarrow \text{PRUNEAIRCRAFT}(\mathbf{H}, \mathbf{r}, L, \hat{S})$ 

```

Phase 3 - Greedy Group

```

15:  $v = 2$ 
16: while  $|L| \geq v$  do
17:    $\text{tmp} = L$ 
18:    $\text{Combinations} = \binom{L}{v}$ 
19:   for each  $C \in \text{Combinations}$  do
20:      $T_C = (L \cup \hat{S}) \setminus \{C\}$ 
21:     if  $\forall S \subseteq C, \sum_{k \in S} r_k \leq R_{C,S}^{T_C} = \log_2 \det \left( \mathbf{I}_M + \dots \right.$ 

$$\left. \frac{P}{N_0} \mathbf{H}_{:S} \mathbf{H}_{:S}^H \left( \mathbf{I}_M + \frac{P}{N_0} \mathbf{H}_{:T_C} \mathbf{H}_{:T_C}^H \right)^{-1} \right)$$

22:       Remove  $C$  from  $L$ 
23:        $S^* \leftarrow \text{add } C$ 
24:     break
25:   if not  $\text{isequal}(\text{tmp}, L)$  then
26:      $v = 1$ 
27:   else
28:      $v = v + 1$ 

```

interference of the outage set, \hat{S} . If $R_l^{\hat{S}} < r_l$, then aircraft l is in outage. This is because the interference caused by the aircraft in \hat{S} cannot be removed from the received signal by any SIC decoding strategy. Therefore, the achievable rate for aircraft l will always be less than or equal to $R_l^{\hat{S}}$. Lemma IV.1 supports this argument, since it indicates that in order to achieve higher rates, the interference on the target signal should be reduced. However, in this case, it is not possible to remove the interference caused by the aircraft already assigned to the outage set \hat{S} . As a result, aircraft l is removed from L and added to \hat{S} . The *PruneAircraft* phase ends when the algorithm can no longer find a new aircraft to add to \hat{S} . The search space for the next step becomes smaller after this phase, since the number of the iterations in the next step depends on the size of L .

The second phase is referred to as *GreedySIC*. This step finds the aircraft that can be successfully decoded using SIC decoders. In line 16 of Algorithm 1, $T_l = L \cup \hat{S} \setminus \{l\}$ is defined as the constraint set of aircraft l and it contains all aircraft in L

and \hat{S} except l . Then, in line 17 of Algorithm 1, $R_l^{T_l}$ is defined as the achievable rate of aircraft l under the interference of T_l . Suppose that the SIC decoder decodes aircraft l treating the aircraft not yet decoded, i.e., T_l , as interference. If $r_l \leq R_l^{T_l}$, then the decoding of aircraft l is successful and the interference caused by aircraft l can be removed from the received signal. Hence, in the subsequent steps, we remove l from L and add it to S^* . This shrinks the constraint set of the remaining aircraft in L . As a result, by Lemma IV.1, the probability of a successful decoding of the remaining aircraft in L increases. Therefore, each time a new aircraft is added to S^* , we retry to decode the remaining aircraft in L under the interference of the shrunk constraint set. This phase ends when all aircraft in the set L hold the condition $R_l^{T_l} < r_l$. This means that there is no SIC decoding order that can successfully decode any of the aircraft in L .

At the end of Algorithm 1, we know that the aircraft in \hat{S} are definitely in outage. The aircraft in L cannot be decoded using only SIC decoders, but they may be decoded when joint group decoders are applied. As a result, the aircraft in S^* form the largest possible S_{SIC}^* . In addition to identifying the elements of optimized S_{SIC}^* , we also find an optimal decoding order for the problem in (13).

B. Group Successive Algorithm (GSA)

GSA is presented in Algorithm 2 and solves the optimization problem given in (8) by considering the joint group decoding options in addition to the SIC scheme. Algorithm 2 (GSA) is an enhancement of Algorithm 1 (SSA). In particular, Algorithm 2 uses the outputs of Algorithm 1 which are: L , S^* , and \hat{S} . The set S^* contains the aircraft that were successfully decoded in the SSA; we assume that their influence on the received signal has been removed and therefore we do not consider these aircraft any further. \hat{S} is the set of aircraft that are certainly in outage. Consequently, we always have to consider the interference caused by these aircraft, but we do not try to decode them. This further narrows the search space. The third set, L , contains the aircraft for which the following condition holds: $\forall l \in L, R_l^{T_l} < r_l \leq R_l^{\hat{S}}$. This means they can achieve the rate r_l under the interference of outage set, \hat{S} , but cannot achieve this rate under the interference of their individual constraint sets, T_l . We try to determine if these aircraft can be decoded jointly as a group, or if they are definitely in outage. In the rest of Algorithm 2, we introduce a new set C to represent a combination of v aircraft from L , such that $C \in \binom{L}{v}$, and hence $|C| = v$.

We refer to the next phase of Algorithm 2 as *PruneSubsets*. It identifies the aircraft that are definitely in outage, thereby minimizing the size of L . In this phase, the algorithm evaluates all aircraft combinations in L of size 2, i.e., $v = 2$. For given $C \subseteq L$, where $|C| = 2$, $R_C^{\hat{S}}$ is defined in line 8 of Algorithm 2. Hence, $R_C^{\hat{S}}$ is the achievable sum rate of aircraft in C under the interference of the outage set, \hat{S} .

Lemma V.1. Let $C = \{o, p\}$, where both aircraft o and p transmit at rate r_o and r_p , respectively, and \hat{S} is the outage set, i.e., users in \hat{S} are certainly in outage. If $R_o^{\hat{S}} \geq r_o$, $R_p^{\hat{S}} \geq r_p$, and $R_C^{\hat{S}} < r_o + r_p$, then both o and p are in outage.

Proof. We define $\hat{S}_p = \{o\} \cup \hat{S}$ and $\hat{S}_o = \{p\} \cup \hat{S}$. From (6), we have the following relationship

$$R_C^{\hat{S}} = R_p^{\hat{S}_p} + R_o^{\hat{S}} = R_o^{\hat{S}_o} + R_p^{\hat{S}}. \quad (15)$$

We are given the following inequalities

$$R_o^{\hat{S}} \geq r_o, R_p^{\hat{S}} \geq r_p, \text{ and } R_C^{\hat{S}} < r_o + r_p. \quad (16)$$

From $R_C < r_o + r_p$, we can conclude that the joint group decoding of aircraft o and p is not possible. Moreover, using the given inequalities, we can derive the following:

$$\begin{aligned} R_C^{\hat{S}} - R_p^{\hat{S}} &= R_o^{\hat{S}_o} < r_o, \\ R_C^{\hat{S}} - R_o^{\hat{S}} &= R_p^{\hat{S}_p} < r_p. \end{aligned} \quad (17)$$

These inequalities imply that neither aircraft o nor aircraft p can be decoded under each other's interference. Therefore, both aircraft are in outage. \square

We know that $\forall l \in L, r_l \leq R_l^{\hat{S}}$. By Lemma V.1, if $R_C^{\hat{S}} < \sum_{k \in C} r_k$, then the aircraft in C are in outage. These aircraft are then removed from L and added to \hat{S} . As the number of aircraft in \hat{S} increases, some aircraft in L may no longer satisfy the condition: $r_l \leq R_l^{\hat{S}}$. Therefore, each time new aircraft are added to \hat{S} , we stop evaluating the remaining aircraft combinations of size 2 (see line 12 of Algorithm 2). We then use the *PruneAircraft* function (see line 14 of Algorithm 2) in order to check if the condition $r_l \leq R_l^{\hat{S}}$ still holds for all remaining aircraft in L with the updated \hat{S} . If the condition does not hold for an aircraft, it means the aircraft is in outage, so it is removed from L and added to \hat{S} . The *PruneAircraft* function stops once it can no longer identify any new aircraft in outage. Afterwards, we generate new combinations of size 2 from the remaining aircraft in L and repeat the process from the beginning. The *PruneSubsets* phase ends either when we can no longer find a new aircraft to add to \hat{S} or when $|L| \leq 1$. By reducing the number of aircraft in L , we significantly lower the computational complexity of the next phase.

The final phase of Algorithm 2 is called *GreedyGroup*. In this step, the remaining aircraft in L are evaluated. The set C represents one combination of v aircraft in L , i.e., $C \in \binom{L}{v}$, and hence $|C| = v$. Initially, v is set to 2 in line 15 of Algorithm 2, the value of v changes during the course of the function. In line 20 of Algorithm 2, $T_C = (L \cup \hat{S}) \setminus \{C\}$ is defined as the constraint set of C and contains all aircraft in L and \hat{S} except C . $R_{C,S}^{T_C}$ is defined in line 21 of Algorithm 2 as the achievable sum rate of aircraft in S , which is a subset of C , under the interference of T_C . For a given value of v and L , there are two possibilities:

- 1) If $\forall S \subseteq C, \sum_{l \in S} r_l \leq R_{C,S}^{T_C}$, then the aircraft in C can be decoded successfully, and their interference can be cancelled. To this end, we remove the aircraft in C from L and add them to S^* . It is important to note that this condition is equivalent to the one given in (9), where C is defined by S^* and T_C is defined by \hat{S} . Moreover, by Lemma IV.1, removing aircraft in C from L increases the probability of successful decoding for the remaining aircraft in L , as it reduces the number of aircraft in

their individual constraint set. Therefore, each time some aircraft are removed from L , we break the *for-loop* on line 24 of Algorithm 2 and change the value of v to 1, as shown on line 26. Setting v to 1 corresponds to considering a SIC decoder. This change in the value of v is made because, with the shrunken constraint set, some aircraft in L may now be decoded using the SIC decoder.

- 2) If none of the combinations of v aircraft in L satisfy the condition $\forall S \subseteq C, \sum_{l \in S} r_l \leq R_{C,S}^{T_C}$, i.e., there is no group C with size v in L that can be successfully decoded, then we increment the value of v by one, as shown on line 28 of Algorithm 2. Increasing the value of v means that we now consider decoding the aircraft in L in a larger group.

In summary, the value of v changes in two scenarios during the *GreedyGroup* phase: First, whenever some aircraft are removed from L and added to S^* , then v is set to 1. Second, if we cannot find any group of aircraft that can be successfully decoded at the current value of v , then v is incremented by 1, i.e., $v = v + 1$. The *GreedyGroup* phase ends either when $|L| = 0$, meaning all K aircraft have been already assigned to either S^* or \hat{S} , or when $|L| < v$, indicating that the aircraft in L are certainly in outage, along with the aircraft in \hat{S} . With Algorithm 2, we find the optimal set S^* for the problem given in (8). The proof is given in Appendix A.

C. Limited Group Successive Algorithm (LGSA)

The implementation of joint group decoders comes at the cost of high complexity, and as a result, joint group decoding of large groups of aircraft may not be feasible in real-world applications for the time being. LGSA addresses this by limiting the number of aircraft that can be decoded jointly, which is achieved by a modification of Algorithm 2 (GSA). In LGSA, the *while-loop* condition in line 16 of Algorithm 2 is modified from $|L| \geq v$ to $v_{\max} \geq v$. This change forces the algorithm to ensure that group sizes remain less than or equal to v_{\max} . While this reduces the complexity, it comes at the expense of a higher outage probability.

VI. LITERATURE REVIEW OF EXISTING DECODING ORDERING STRATEGIES

The outage probability of SIC decoders depends on the decoding order, as explained in Section IV. To this end, in this section we present two decoding order strategies from the literature and compare their performance with SSA in Section VII. The first is V-BLAST [24], which is a prominent decoding order in the literature. The second is the decoding order proposed in [25], which is based on the channel gain and transmission rate (CGTR) of the aircraft.

The set of non-outage aircraft for a given decoding order, $i_1 \rightarrow i_2 \rightarrow \dots \rightarrow i_K$, is defined as S_{DO}^* . Algorithm 3 shows how to determine S_{DO}^* . In line 3 of Algorithm 3, the aircraft that interferes with the i_u -th aircraft is defined as F_u . The achievable rate for the aircraft i_u , $R_{i_u}^{F_u}$, is obtained using (11), where F_u corresponds to T_u . By simulating the aircraft positions multiple times, we compute the outage probability, $P_{\text{out}}^{\text{DO}} = 1 - \frac{\mathbb{E}[|S_{\text{DO}}^*|]}{K}$.

Algorithm 3 Non-Outage Aircraft for a Given Decoding Order

```

1:  $\hat{S} = \emptyset$ 
2: for  $u = 1, 2, \dots, K$  do
3:    $F_u = \hat{S} \cup \{i_{u+1}, \dots, i_K\}$ 
4:   if  $r_{i_u} \leq R_{i_u}^{F_u}$  then
5:      $S_{\text{DO}}^* \leftarrow \text{add } i_u$ 
6:   else
7:      $\hat{S} \leftarrow \text{add } i_u$ 

```

A. V-BLAST

V-BLAST maximizes the minimum signal-to-noise-interference-ratio (SINR) at the detector output, by decoding the signal with the highest SINR at each iteration [24].

Lemma VI.1. *If $r_k = r_G, \forall k \in \{1, 2, \dots, K\}$, then an optimal decoding order of the optimization problem given in (13) is decoding the aircraft with the highest SINR at each step of the SIC process.*

Proof. Let o and p be any two aircraft and $T_{o,p}$ be the set of all the other aircraft that have not yet been successfully decoded. Accordingly, we define T, T_o, T_p as follows

$$\begin{aligned}
T &= \{o, p\} \cup T_{o,p}, \\
T_o &= \{p\} \cup T_{o,p}, \\
T_p &= \{o\} \cup T_{o,p}.
\end{aligned} \tag{18}$$

By Lemma IV.1, $R_p^{T_o,p} \geq R_p^{T_p}$ and $R_o^{T_o,p} \geq R_o^{T_o}$, since $T_{o,p}$ is a subset of T_p and T_o . We consider two decoding orders:

- *Decoding order 1:* $p \rightarrow o \rightarrow T_{o,p}$
The achievable rate for aircraft p , $R_p^{T_p}$, and in the case of successful decoding of aircraft p , the achievable rate for aircraft o is $R_o^{T_o,p}$.
- *Decoding order 2:* $o \rightarrow p \rightarrow T_{o,p}$
The achievable rate for aircraft o , $R_o^{T_o}$, and in the case of successful decoding of aircraft o , the achievable rate for aircraft p is $R_p^{T_o,p}$.

Let us assume that $R_o^{T_o} \geq R_p^{T_p} \geq R_k^{T_k}, \forall k \in T_{o,p}$ where $T_k = T \setminus \{k\}$, which contains all elements of T except k . This means that aircraft o has the highest SINR followed by p . There are three possibilities:

- *Possibility 1:* $R_o^{T_o} \geq R_p^{T_p} \geq r_G$
Both decoding orders can successfully decode aircraft o and p , since $R_p^{T_o,p} \geq R_p^{T_p}$ and $R_o^{T_o,p} \geq R_o^{T_o}$. As a result, $\{o, p\} \in S_{\text{MMSE-SIC}}^*$.
- *Possibility 2:* $r_G \geq R_o^{T_o} \geq R_p^{T_p}$
Neither of the decoding orders can decode the first aircraft that needs to be decoded. Moreover, given that $R_o^{T_o} \geq R_p^{T_p} \geq R_k^{T_k}, \forall k \in T_{o,p}$ no other aircraft in T can be successfully decoded with any other decoding order.
- *Possibility 3:* $R_o^{T_o} \geq r_G \geq R_p^{T_p}$

- *Decoding order 1* cannot decode aircraft p , so the interference caused by p cannot be removed. Aircraft o can be decoded under the interference of p . All the aircraft in $T_{o,p}$ must be decoded under the interference of p , which reduces their chances of successful decoding.

- *Decoding order 2* can decode aircraft o . Since $R_p^{T_{o,p}} \geq R_p^{T_p}$, there is a chance that aircraft p might also be successfully decoded. If $r_G \geq R_p^{T_{o,p}} \geq R_p^{T_p}$, then the results will be the same as *decoding order 1*. However, if $R_p^{T_{o,p}} \geq r_G \geq R_p^{T_p}$, then aircraft p can be successfully decoded, and the aircraft in $T_{o,p}$ will be decoded in the absence of interference from o and p . This increases the probability of their successful decoding.

Based on the analysis of these three possibilities, the outcome of the decoding orders differs only in *possibility 3*. In this case, *decoding order 2* clearly leads to better results. Therefore, for this given problem, the optimal decoding order is to decode the aircraft with the highest SINR at each iteration. \square

By Lemma VI.1 we can claim that V-BLAST finds an optimal solution for the problem given in (13), for an equal-rate system, but it may not find the optimal solution for the variable-rate system.

B. Channel Gain and Transmission Rate (CGTR)

In [25], the decoding order problem is studied for a power-controlled system, where users could transmit at different power levels in order to optimize the sum rate of the system. The authors of [25] assume that each user must meet a certain minimum rate. While the minimum rate requirement is similar to our scenario, we do not consider a power-controlled system. This is because having aircraft with different transmit powers is not a viable option in ATM systems due to regulatory constraints [5].

In [25], the decreasing order of $|\mathbf{h}_{:k}|^2(1 + \frac{1}{2^{r_k+1}})$ is proposed as the optimal decoding order to maximize the sum rate, i.e., $\max_{\Pi} \sum_{k \in S_{\text{SIC}}^*} r_k$. For an equal-rate system, this decoding order leads to decreasing order of $|\mathbf{h}_{:k}|^2$ since $(1 + \frac{1}{2^{r_k+1}})$ becomes a constant. Moreover, in an equal-rate system, optimizing the sum rate minimizes the outage probability, which aligns with our objective.

Despite the fact that the study in [25] does not explicitly mention the number of antenna elements on the receiver, their approach applies only to single antenna receivers and cannot be used for multiple antenna receivers, since the linear dependencies between the users' channel vectors are not considered. In the multiple antenna NOMA concept, the interference caused by one user to another depends not only on the power of the interfering signal but also on the linear dependence of the users' channel vectors. If the channel vectors are orthogonal, there will be no interference. However, if the channel vectors are linearly dependent, then there can be significant interference.

VII. NUMERICAL RESULTS AND DISCUSSION

In this section, we evaluate the performance of the proposed algorithms, SSA, GSA, and LGSA. We also compare their performance with the decoding ordering strategies from [24] and [25]. Evaluations are performed for two types of systems: equal-rate and variable-rate. In an equal-rate system, all aircraft transmit at the guaranteed rate, r_G , of the

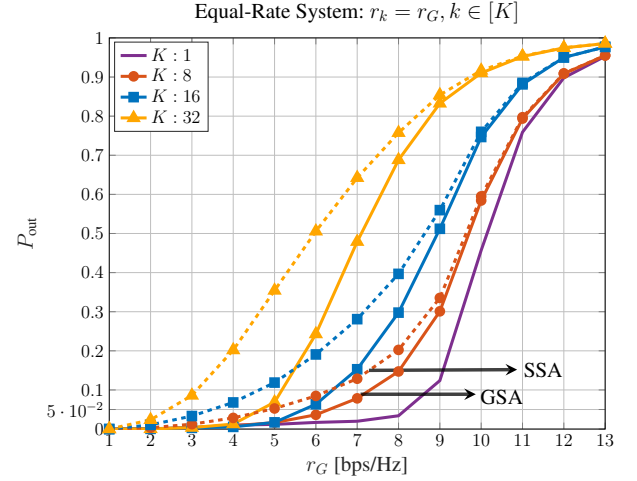


Fig. 3. Outage probability, P_{out} , for an equal-rate system. The results are obtained for a UPRA with $M = 64$ and for varying number of aircraft, K . The dashed line represents SSA and the solid line corresponds to GSA.

system, i.e., $r_k = r_G, \forall k \in [K]$, where $[K] = \{1, 2, \dots, K\}$. This approach allows us to understand the relationship between the transmission rate and the outage probability, P_{out} , and to analyze the range of rates that could be supported in the given geometry-based stochastic channel model. Based on these results, we determine the transmission rate range in variable-rate simulations. Accordingly, in variable-rate simulations we focus on the relationship between the number of aircraft sharing a non-orthogonal channel, K , and P_{out} . Finally, we evaluate the computational complexity of the proposed algorithms and compare them to a brute-force approach. The results are obtained for a UPRA with $M = 64$.

A. Evaluation of Proposed Algorithms: SSA, GSA and LGSA

Figure 3 compares the achievable outage probabilities using SSA and GSA for an equal-rate system. As the aircraft number, K , increases, the difference in performance between SSA and GSA gets larger. This means that joint group decoding of the aircraft becomes more and more necessary to maintain a low P_{out} at larger values of K . For a fixed P_{out} , the system's sum rate capacity can be determined by multiplying K and r_G . For example, at $P_{\text{out}} = 0.05$ in Fig. 3, the sum rate for $K = 1$ is approximately 8.2 bps/Hz, whereas for $K = 32$ using the GSA algorithm, the sum rate is approximately $32 \cdot 4.5$ bps/Hz = 144 bps/Hz. As a result, while the lower values of K allow for a higher r_G at a fixed P_{out} , the sum rate increases at larger values of K .

The evaluation of LGSA is only meaningful if there is a significant difference between SSA and GSA, as this indicates that GSA achieves low P_{out} values by joint group decoding of aircraft. At this point, LGSA becomes relevant, as it ensures that the number of aircraft decoded together remains below the limit, v_{max} . This allows LGSA to offer a joint decoding approach that is more practical for real-world applications. In Fig. 4, P_{out} is computed for $K = 32$ in an equal-rate system. LGSA is evaluated for two group size limits, $v_{\text{max}} = 2$ and $v_{\text{max}} = 4$. For $v_{\text{max}} = 2$, LGSA and GSA exhibit nearly identical outage probabilities for $r_G \leq 3$ [bps/Hz]. For

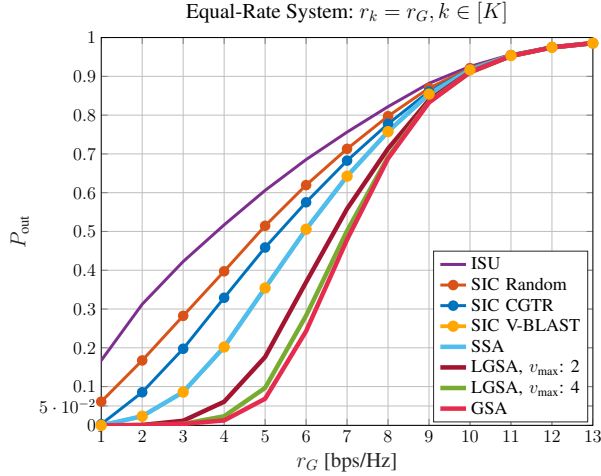


Fig. 4. Outage probability, P_{out} vs. guaranteed rate r_G for $K = 32$ in an equal-rate system. The results are obtained for a UPRA with $M = 64$.

$v_{\text{max}} = 4$, LGSA achieves results nearly identical to GSA for almost all values of r_G .

We define single-user single antenna systems as those where both the GS and the aircraft are equipped with a single antenna, and the aircraft are separated in time or frequency, i.e., orthogonal multiple access (OMA). It is not realistic to expect that all current single-user single antenna GSs worldwide will be replaced by the new multiple antenna GSs simultaneously. In this case, r_G will be defined based on the single-user single antenna GSs to ensure that flight critical messages can also be supported in these stations. For a single-user single antenna system, the P_{out} at a rate of 2 bps/Hz is 0.06, and it increases very steeply for increasing values of r_G . If all aircraft would transmit at the guaranteed rate of a single-user single antenna system, i.e., approximately 2 bps/Hz, the full potential of the installed multiple antenna systems would not be utilized, thereby wasting valuable resources. As shown in Fig. 3 and Fig. 4, the proposed algorithms, SSA, GSA, and LGSA, are capable of achieving higher transmission rates while maintaining a low outage probability. This motivates us to consider a variable-rate system where aircraft transmit at least at the guaranteed rate, but could transmit at higher rates to take full advantage of the multiple antenna systems.

In the variable-rate system, we set r_G to 2 bps/Hz, which is based on the single-user single antenna system where P_{out} is 0.06. Accordingly, the transmission rate of aircraft k is randomly selected from a uniform distribution between 2 and 6 bps/Hz, i.e., $r_k \sim \mathcal{U}(2, 6), \forall k \in [K]$. In Fig. 5, P_{out} is computed for increasing values of K in a variable-rate system. It can be observed that LGSA with $v_{\text{max}} = 2$ has almost the same performance as GSA up to $K = 20$, and LGSA with $v_{\text{max}} = 4$ has the same performance up to $K = 32$. Moreover, LGSA outperforms SSA by a clear margin. These results show that even when joint group decoding is used for groups of only 2, the outage probability can still be significantly reduced compared to SSA, especially for large values of K . In this paper, aircraft are randomly assigned transmission rates during the variable-rate simulations. However, the performance of the system can be improved by determining transmission rates based on factors such as the power of the received signal or

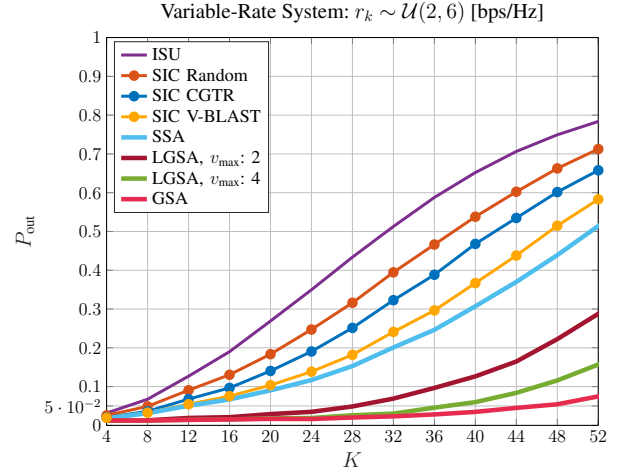


Fig. 5. Outage probability, P_{out} , for a variable-rate system where r_k is uniformly distributed between 2 and 6 bps/Hz. The results are obtained for a UPRA with $M = 64$.

the distance between the aircraft and the GS.

B. Performance Comparison: Proposed Algorithms vs. Existing Decoding Strategies

The outage probability of the ISU decoders and of the SIC decoding order strategies proposed in [24] and [25] are also plotted in Fig. 4 and Fig. 5. In both figures, the minimal outage probability for ISU decoders is notably very high. To achieve a low P_{out} with ISU decoders, the number of simultaneously transmitting aircraft, K , must be very small compared to M . Comparing the ISU decoders with the SIC decoders, we observe that the SIC scheme allows more aircraft to transmit over a non-orthogonal channel with lower outage probabilities. As a result, these findings demonstrate how the SIC scheme reduces the outage probability while also increasing the spectral efficiency when compared to the ISU decoders.

SSA obtains the optimal decoding order for the SIC ordering problem given in (13). In order to demonstrate the importance of the decoding order, we first present the results for a random decoding order in Fig. 4 and Fig. 5, denoted as SIC random. Not surprisingly, SIC random shows the worst performance, with a clear margin between SIC random and SSA in both Fig. 4 and Fig. 5. The decoding order strategy proposed in [25], SIC CGTR, has the worst performance after SIC random in both Fig. 4 and Fig. 5. The authors of [25] argued that they propose an optimal decoding order for a power-controlled system. Although not explicitly stated in [25], their approach is only applicable to single antenna receivers and not to multiple antenna receivers. This is because the linear dependencies between the users' (aircraft's) channel vectors are ignored when calculating the achievable rates. Lastly, we evaluate the well-known V-BLAST [24]. As proved in Lemma VI.1 and shown in Fig. 4, this results in an optimal decoding order when the users transmit at the same rate. For all channel realizations, the set of successfully decoded aircraft by V-BLAST is the same as that of SSA. However, in the variable-rate system, as can be seen in Fig. 5, SSA outperforms V-BLAST.

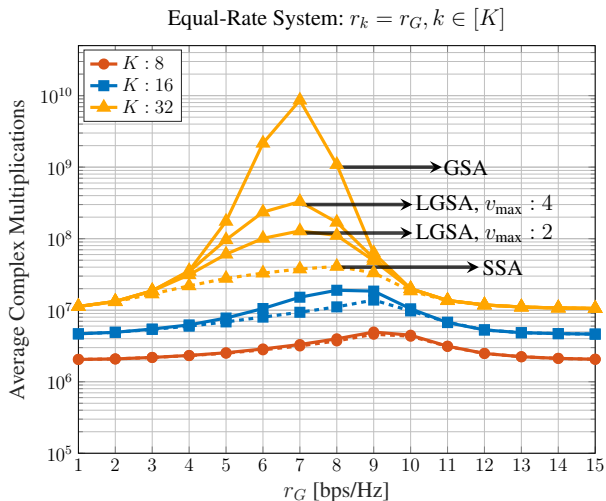


Fig. 6. The average complex multiplications required to compute outage probability, P_{out} , for an equal-rate system. The dashed line represents SSA and the solid line is used for LGSA and GSA. The results are obtained for a UPRA with $M = 64$.

C. Computational Complexity of the Proposed Algorithms

Next, we evaluate the computational complexity of the proposed algorithms based on the average number of complex multiplications required for a given channel matrix and rate point. This is computed based on [35], where the multiplication of a $M \times K$ matrix with a $K \times M$ matrix costs M^2K multiplications and the inverse of an $M \times M$ matrix costs M^3 multiplications.

Figure 6 shows the results for an equal-rate system and Fig. 7 presents the results for a variable-rate system. In both cases the computational complexity increases with K . In Fig. 6, there is a notable peak at $r_G = 7$ bps/Hz for GSA when $K = 32$. In this specific case, many users can be decoded under the interference of the outage set. However, only a few aircraft can achieve 7 bps/Hz under the interference of their constraint set. This results in many aircraft remaining in L during the *GreedyGroup* phase of Algorithm 2 (GSA), which significantly increases the computational load. Nevertheless, for $r_G = 7$ bps/Hz with GSA and $K = 32$, the equal-rate system ends up with a P_{out} of about 0.5 (see Fig. 4). The computational complexity for r_G values that achieve a P_{out} of less than 0.05 is particularly relevant to our analysis. In these cases, the average number of complex multiplications per channel matrix remains below $1 \cdot 10^8$ in Fig. 6. Similarly, in Fig. 7, the average number of complex multiplications remains below $1 \cdot 10^8$ for $K \leq 36$.

If we had to compute the number of aircraft in outage using a brute-force approach for $K = 32$, according to (10) we would have to evaluate (9) $1.8 \cdot 10^{15}$ times for a given channel matrix and a rate point. This would cost about $1.2 \cdot 10^{23}$ complex multiplications. For example, suppose we use a very powerful processor with a clock rate of 9 GHz and each complex multiplication takes one clock cycle. Then it would take us about 300 years to compute the number of aircraft in outage for a given channel matrix and a rate point with a brute-force approach. By comparison, the calculation of the $1 \cdot 10^8$ complex multiplications on the same processor would take about 0.01 s.

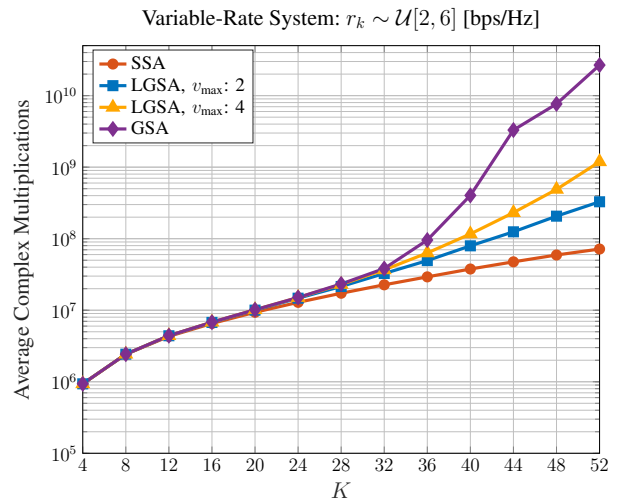


Fig. 7. The average complex multiplications required to compute outage probability, P_{out} , for a variable-rate system, where r_k is uniformly distributed between 2 and 6 bps/Hz. The results are obtained for a UPRA with $M = 64$.

VIII. CONCLUSION AND OUTLOOK

In this paper, we investigate the multiuser multiple antenna systems using the non-orthogonal multiple access (NOMA) concept while employing a realistic air-ground (AG) channel model. We explore the interplay between the capacity region and the outage probability and demonstrate that the outage probability is the relevant performance metric for the AG channel. We then show that the outage probability depends on the decoding technique, where three decoding techniques are considered: independent single-user (ISU) decoders, successive interference cancellation (SIC) decoders, and joint group decoders. While the outage probability calculation is relatively straightforward for ISU decoders, this is not the case for the SIC decoders and the joint group decoders. We therefore propose three algorithms to calculate the outage probability for SIC decoders and joint group decoders. These algorithms not only compute the upper bound on the minimum achievable outage probability for a given decoding approach, but also derive practical strategies for the implementation of these decoding strategies.

The first algorithm is the single successive algorithm (SSA), which identifies the optimal decoding order that minimizes the outage probability for SIC decoders. We show that SSA outperforms the SIC decoding ordering proposed in [25]. Furthermore, we prove and demonstrate that the SIC decoding ordering proposed in V-BLAST [24], obtains an optimal solution when all the aircraft transmit at the same rate. However, when a variable-rate system is considered, we show that SSA outperforms V-BLAST [24]. Additionally, the results show that the SIC decoders significantly increase the spectral efficiency compared to the ISU decoders.

The second algorithm is the group successive algorithm (GSA), which enhances SSA by using SIC decoders together with joint group decoders. GSA significantly improves the spectral efficiency when compared to SSA by allowing a large number of aircraft to transmit over a non-orthogonal channel with a very low outage probability. One concern with GSA is its feasibility in real-world applications, since joint decoding

of a large group of aircraft might not be viable at the time being. To address this concern, we propose the limited group successive algorithm (LGSA). While LGSA does not obtain the optimal solution, it does restrict the group of aircraft that will be decoded jointly. Even when the largest group of aircraft is limited to two, the results show that LGSA leads to a significant reduction in the probability of outage as compared to the minimum outage probability obtainable with SIC-only decoders such as SSA.

As a result, LGSA shows great promise. In our future work, we will combine the receiver strategies for multiuser joint decoding proposed in [36], [37] with the decoding order obtained through LGSA.

APPENDIX A

PROOF OF THE OPTIMALITY OF ALGORITHM 2

Algorithm 2, GSA, solves the problem given in (8) by finding the maximal set S^* that satisfies the condition given in (9). It concludes with three sets: S^* , \hat{S} , and L . In Section V, in the explanation of the algorithm, it is justified that the aircraft in \hat{S} are definitively in outage. Additionally, it is verified that the aircraft in S^* can be successfully decoded. In this case, to show that GSA identifies the largest set of aircraft that can be successfully decoded, it must be proved that all aircraft remaining in L , if any, are definitely in outage.

The algorithm terminates in two cases: either when $|L| = 0$, or when $|L| < v$. In the case where $|L| = 0$, it follows trivially that S^* is the optimal set. Therefore, we focus on the scenario where $|L| \geq 1$. Before terminating, the algorithm ensures that none of the combinations of L aircraft satisfy the condition $\forall S \subseteq C, \sum_{k \in S} r_k \leq R_{C,S}^{T_C}$, i.e.,

$$\forall v \in \{1, \dots, |L|\}, \forall C \in \binom{L}{v}, \quad \neg \left(\forall S \subseteq C, \sum_{k \in S} r_k \leq R_{C,S}^{T_C} \right), \quad (19)$$

where \neg indicates the *not* operator. This is equivalent to: for all combinations of aircraft in L , there exists at least one subset S such that the condition $S \subseteq C, \sum_{k \in S} r_k > R_{C,S}^{T_C}$ holds, i.e.,

$$\forall v \in \{1, \dots, |L|\}, \forall C \in \binom{L}{v}, \quad \exists S \subseteq C \text{ such that } \sum_{k \in S} r_k > R_{C,S}^{T_C}. \quad (20)$$

As a result, there are no aircraft in L that can be decoded by either SIC or joint group decoders, regardless of the group size. Therefore, all the aircraft in L are definitively in outage, and S^* is the optimal set.

REFERENCES

- [1] "Performance review report 2023," EUROCONTROL, Tech. Rep., 2024.
- [2] "Communications operating concept and requirements for the future radio system," EUROCONTROL & FAA, Tech. Rep. version 2, 2007.
- [3] N. Fistas, "Future aeronautical communications: The data link component," in *Future Aeronautical Communications*, S. Plass, Ed. Rijeka: IntechOpen, 2011, ch. 11. [Online]. Available: <https://doi.org/10.5772/29899>
- [4] "Comparison of typical air/ground aeronautical communication system propagation losses in the L band and the C band," ICAO, Tech. Rep., 2005.
- [5] "Report on the results of the ITU world radio communication conference (WRC)," ICAO, Tech. Rep., 2007. [Online]. Available: [https://www.icao.int/safety/acp/repository/an.2007.wp.8284.en\[1\].pdf](https://www.icao.int/safety/acp/repository/an.2007.wp.8284.en[1].pdf)
- [6] SESAR. [Online]. Available: <https://www.sesarju.eu/>
- [7] NextGen. [Online]. Available: <http://www.faa.gov/nextgen>
- [8] A. Gürbüz, A. Steingass, and D. Becker, "On the cost-effectiveness of using beamforming at the ground station for aeronautical communications," in *2024 18th European Conference on Antennas and Propagation (EuCAP)*, 2024, pp. 1–5.
- [9] D. Gesbert, M. Kountouris, R. W. Heath, C.-b. Chae, and T. Salzer, "Shifting the MIMO paradigm," *IEEE Signal Processing Magazine*, vol. 24, no. 5, pp. 36–46, 2007.
- [10] G. Caire and S. Shamai, "On the achievable throughput of a multiantenna Gaussian broadcast channel," *IEEE Transactions on Information Theory*, vol. 49, no. 7, pp. 1691–1706, 2003.
- [11] T. L. Marzetta, "Noncooperative cellular wireless with unlimited numbers of base station antennas," *IEEE Transactions on Wireless Communications*, vol. 9, no. 11, pp. 3590–3600, 2010.
- [12] E. Larsson, F. Tufvesson, O. Edfors, and T. Marzetta, "Massive MIMO for next generation wireless systems," *Submitted to IEEE Commun. Mag.*, vol. 52, 04 2013.
- [13] X. Wang, H. Chen, and F. Tan, "Hybrid OMA/NOMA mode selection and resource allocation in space-air-ground integrated networks," *IEEE Transactions on Vehicular Technology*, vol. 74, no. 1, pp. 699–713, 2025.
- [14] Y. Dong, G. Xu, N. Zhao, Q. Zhang, Z. Song, and W. Zhang, "Outage performance of NOMA-based multi-user satellite communication system under polarization conversion," *IEEE Transactions on Vehicular Technology*, vol. 74, no. 3, pp. 5146–5151, 2025.
- [15] X. Li, M. Zhang, H. Chen, C. Han, L. Li, D.-T. Do, S. Mumtaz, and A. Nallanathan, "UAV-enabled multi-pair massive MIMO-NOMA relay systems with low-resolution ADCs/DACs," *IEEE Transactions on Vehicular Technology*, vol. 73, no. 2, pp. 2171–2186, 2024.
- [16] J. Rasool, G. E. Oien, J. E. Hakegard, and T. A. Myrvoll, "On multiuser MIMO capacity benefits in air-to-ground communication for air traffic management," in *2009 6th International Symposium on Wireless Communication Systems*, 2009, pp. 458–462.
- [17] G. Caire, "On the ergodic rate lower bounds with applications to massive MIMO," *IEEE Transactions on Wireless Communications*, vol. 17, no. 5, pp. 3258–3268, 2018.
- [18] N. Schneckenburger, T. Jost, D. Shutin, M. Walter, T. Thiasiriphet, M. Schnell, and U.-C. Fiebig, "Measurement of the L-band air-to-ground channel for positioning applications," *IEEE Transactions on Aerospace and Electronic Systems*, vol. 52, no. 5, pp. 2281–2297, 2016.
- [19] D. W. Matolak and R. Sun, "Air-ground channel characterization for unmanned aircraft systems—part I: Methods, measurements, and models for over-water settings," *IEEE Transactions on Vehicular Technology*, vol. 66, no. 1, pp. 26–44, 2017.
- [20] R. Sun and D. W. Matolak, "Air-ground channel characterization for unmanned aircraft systems part II: Hilly and mountainous settings," *IEEE Transactions on Vehicular Technology*, vol. 66, no. 3, pp. 1913–1925, 2017.
- [21] N. Schneckenburger, T. Jost, M. Walter, G. del Gaudio, D. W. Matolak, and U.-C. Fiebig, "Wideband air-ground channel model for a regional airport environment," *IEEE Transactions on Vehicular Technology*, vol. 68, no. 7, pp. 6243–6256, 2019.
- [22] A. Gürbüz and M. Walter, "An air-ground channel modeling approach for multiple antenna systems," in *2023 Integrated Communication, Navigation and Surveillance Conference (ICNS)*, 2023, pp. 1–9.
- [23] EECNS Team, "SESAR2020 PJ14-02-01 - LDACS A/G Specification," SESAR Joint Undertaking, Tech. Rep., 2019.
- [24] P. Wolniansky, G. Foschini, G. Golden, and R. Valenzuela, "V-BLAST: an architecture for realizing very high data rates over the rich-scattering wireless channel," in *1998 URSI International Symposium on Signals, Systems, and Electronics. Conference Proceedings (Cat. No.98EX167)*, 1998, pp. 295–300.
- [25] J. Zhang, L. Zhu, Z. Xiao, X. Cao, D. O. Wu, and X.-G. Xia, "Optimal and sub-optimal uplink NOMA: Joint user grouping, decoding order, and power control," *IEEE Wireless Communications Letters*, vol. 9, no. 2, pp. 254–257, 2020.
- [26] H. Moritz, "Geodetic reference system," *Bull. Geodesique*, p. 395–405, 1980.
- [27] M. A. Bellido-Manganell, T. Gräupl, O. Heirich, N. Mäurer, A. Filip-Dhaubhadel, D. M. Mielke, L. M. Schalk, D. Becker, N. Schneckenburger, and M. Schnell, "LDACS flight trials: Demonstration and per-

- formance analysis of the future aeronautical communications system,” *IEEE Transactions on Aerospace and Electronic Systems*, vol. 58, no. 1, pp. 615–634, 2022.
- [28] “Eurocontrol publication for ECAC area rules for OAT-IFR,” <https://www.eurocontrol.int/>, EUROCONTROL, Tech. Rep., 2023, accessed: 2025-04-15.
 - [29] N. Schneckenburger, “A wide-band air-ground channel model,” Ph.D. dissertation, A Wide-Band Air-Ground Channel Model, Februar 2018.
 - [30] L. Ozarow, S. Shamai, and A. Wyner, “Information theoretic considerations for cellular mobile radio,” *IEEE Transactions on Vehicular Technology*, vol. 43, no. 2, pp. 359–378, 1994.
 - [31] J. D. Parsons, *The Mobile Radio Propagation Channel*. Wiley, 2000.
 - [32] *Electrical Characteristics of the Surface of the Earth*, ITU-R P.527-3 Recommendation, 1992.
 - [33] T. M. Cover and J. A. Thomas, *Elements of Information Theory 2nd Edition (Wiley Series in Telecommunications and Signal Processing)*. Wiley-Interscience, July 2006.
 - [34] B. Clerckx and C. Oestges, *MIMO Wireless Networks: Channels, Techniques and Standards for Multi-Antenna, Multi-User and Multi-Cell Systems*, 2nd ed. USA: Academic Press, Inc., 2013.
 - [35] G. H. Golub and C. F. Van Loan, *Matrix Computations*, 4th ed. The Johns Hopkins University Press, 2013.
 - [36] J. Boutros and G. Caire, “Iterative multiuser joint decoding: unified framework and asymptotic analysis,” *IEEE Transactions on Information Theory*, vol. 48, no. 7, pp. 1772–1793, 2002.
 - [37] S. ten Brink, G. Kramer, and A. Ashikhmin, “Design of low-density parity-check codes for modulation and detection,” *IEEE Transactions on Communications*, vol. 52, no. 4, pp. 670–678, 2004.